

PIT Project

Behaviour of steel framed structures under fire conditions

**British Steel Fire Tests:
Analysis of results from BS/TEST3 model,
Part A: Grillage model**

Final Research Report

Report R00 AM4

Abdel Moniem Sanad

**The University of Edinburgh
School of Civil & Environmental Engineering
Edinburgh, UK**

March, 2000

TABLE OF CONTENTS

1. GENERAL NOTES	3
2. LIST OF FIGURES :	3
2.1. General layout	3
2.2. Heated joists	3
PBE__12	3
SB12_EF	4
SB2__EF	4
2.3. Protected joists	4
PBF__12	4
SB1__EF	5
2.4. Transverse slab	5
Rib near the heated Primary beam	5
Rib at mid-span	5
Rib near the edge Primary beam	6
3. INTRODUCTION	7
4. FIGURES DESCRIPTION	9
4.1. Heated joists	9
PBE__12	9
SB12_EF	9
SB2__EF	9
4.2. Protected joists	10
PBF__12	10
SB1__EF	10
4.3. Transverse slab	11
Rib at 0.9m from heated Primary beam	11
Rib at 4.5m from heated Primary beam	11
Rib at 7.2m from heated Primary beam	11
5. CONCLUSION	11
6. REFERENCES	13
7. FIGURES	14

1. GENERAL NOTES

In the description of the numerical model below the following terms are used :

“The plane” to define the plane of the floor.

“Joist” means a steel beam, and the test Joist means the heated Joist during the fire test.

“Vertical” means vertical to the slab plane.

“In plane” means in the plane of the Long. slab.

“Joist longitudinal direction” or “longitudinal direction” to mean parallel to the Joist length coordinate.

“Transverse direction” to mean at right angle to the Joist longitudinal direction (i.e. in the direction of the longitudinal axis of the ribs Figure 1.

“Reference vertical co-ordinate” is the interface between the Long. slab and Joist .

2. LIST OF FIGURES :

2.1. General layout

Figure 1: Layout of the Cardington fire test³.

Figure 2: Layout of the finite element model

2.2. Heated joists

PBE__12

Figure 3: Joist vertical displacement

Figure 4: Joist axial force

Figure 5: Comp. slab axial force

Figure 6: Composite axial force at different location

Figure 7: Joist Shear Force

Figure 8: Comp. slab shear force

Figure 9: Composite shear force at different location

Figure 10: Joist Moment

Figure 11: Comp. slab moment

Figure 12: Composite Moment at different location

Figure 13: P-D effect at different section

Figure 14: Composite moment at mid-span

SB12_EF

- Figure 15: Joist vertical displacement
- Figure 16: Joist axial force
- Figure 17: Comp. slab axial force
- Figure 18: Composite axial force at different location
- Figure 19: Joist Shear Force
- Figure 20: Comp. slab shear force
- Figure 21: Composite shear force at different location
- Figure 22: Joist Moment
- Figure 23: Comp. slab moment
- Figure 24: Composite Moment at different location
- Figure 25: P-D effect at different section
- Figure 26: Composite moment at mid-span

SB2_EF

- Figure 27: Joist vertical displacement
- Figure 28: Joist axial force
- Figure 29: Comp. slab axial force
- Figure 30: Composite axial force at different location
- Figure 31: Joist Shear Force
- Figure 32: Comp. slab shear force
- Figure 33: Composite shear force at different location
- Figure 34: Joist Moment
- Figure 35: Comp. slab moment
- Figure 36: Composite Moment at different location
- Figure 37: P-D effect at different section
- Figure 38: Composite moment at mid-span

2.3. Protected joists

PBF_12

- Figure 39: Joist vertical displacement
- Figure 40: Joist axial force
- Figure 41: Comp. slab axial force
- Figure 42: Composite axial force at different location

Figure 43: Joist Shear Force
Figure 44: Comp. slab shear force
Figure 45: Composite shear force at different location
Figure 46: Joist Moment
Figure 47: Comp. slab moment
Figure 48: Composite Moment at different location
Figure 49: P-D effect at different section
Figure 50: Composite moment at mid-span

SBI_EF

Figure 51: Joist vertical displacement
Figure 52: Joist axial force
Figure 53: Comp. slab axial force
Figure 54: Composite axial force at different location
Figure 55: Joist Shear Force
Figure 56: Comp. slab shear force
Figure 57: Composite shear force at different location
Figure 58: Joist Moment
Figure 59: Comp. slab moment
Figure 60: Composite Moment at different location
Figure 61: P-D effect at different section
Figure 62: Composite moment at mid-span

2.4. Transverse slab

Rib near the heated Primary beam

Figure 63: Vertical displacement along the rib
Figure 64: Rib moment during fire
Figure 65: Rib shear force during fire
Figure 66: Rib axial force during fire

Rib at mid-span

Figure 67: Vertical displacement along the rib
Figure 68: Rib moment during fire
Figure 69: Rib shear force during fire

Figure 70: Rib axial force during fire

Rib near the edge Primary beam

Figure 71: Vertical displacement along the rib

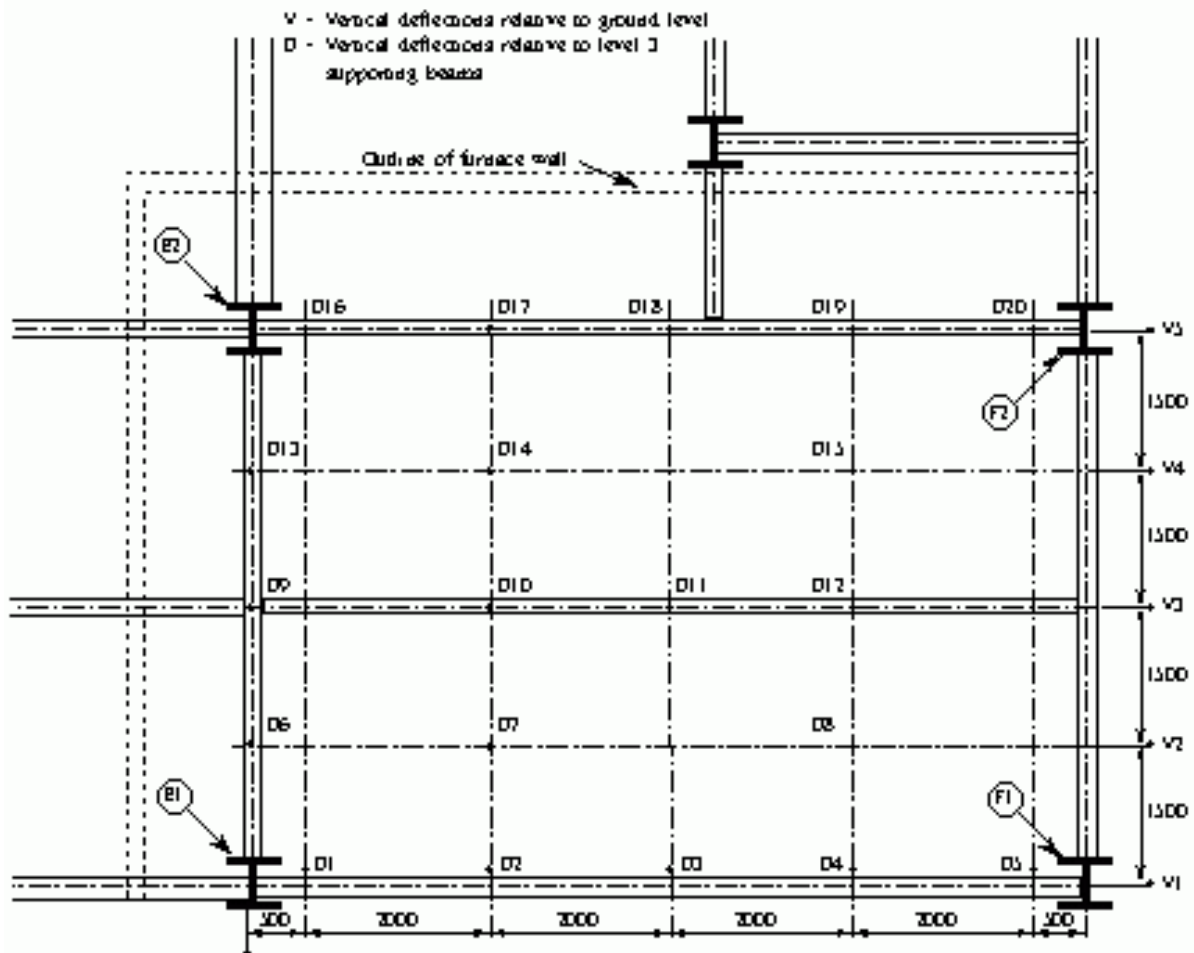
Figure 72: Rib moment during fire

Figure 73: Rib shear force during fire

Figure 74: Rib axial force during fire

3. INTRODUCTION

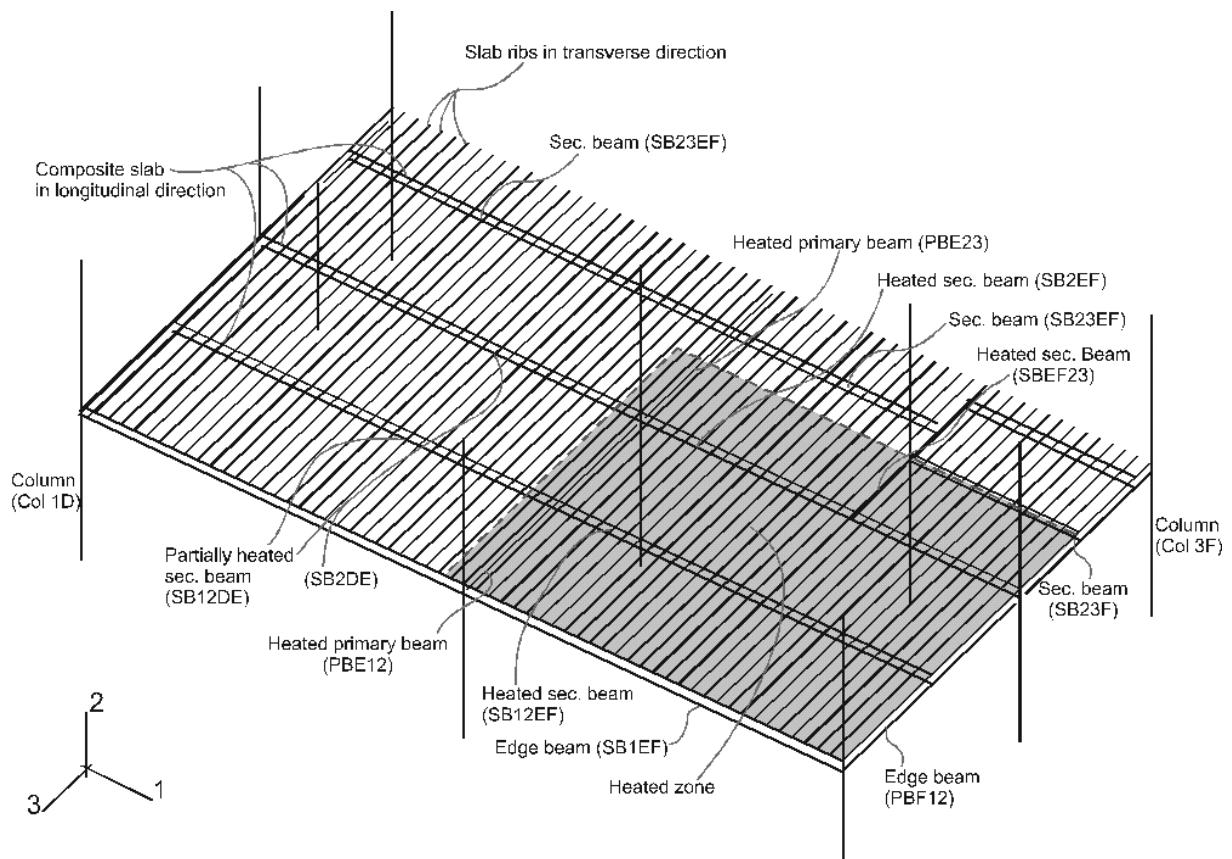
The following report discusses of the structural behaviour during the Cardington fire test³. The results discussed in this report are obtained from the finite element model developed at the University of Edinburgh (Sanad 2000)¹². The geometry and layout of the test compartment are given in Figure 1. The test is fully described in (Kirby 1995)⁷. Test 3 was performed on the second floor of the building and the fire compartment was arranged to study the behaviour of the structure under a corner fire condition. The dimensions of the compartment were 10m×8m. The tested secondary beams had a span of 9m, and was connected to columns or to primary beams at their ends. A standard composite profiled deck slab was used to span the 3m between equally spaced secondary beams supported either from primary beams or columns (Bravery 1993)¹. The slab was cast in-situ on profiled steel decking and had a total thickness of 130mm. The thickness of the steel deck used is 9mm and the reinforcement consists of one layer of A142.



Layout of Test3

Figure 1

The finite element model was fully described in (Sanad 1999)¹². Figure 2 shows the layout of half the test compartment where the tested joist spanning 9m between two columns and the slab ribs crossing it at different locations. In the following section a discussion of the structural behaviour during the test is given based on the output obtained from the numerical model. The main forces and moment plotted for the tested joist and the slab were obtained directly from calculation. The composite forces and composite moment were subject to a more elaborated data processing. The composite axial force over the beam is the sum of the axial force in the joist and the composite longitudinal slab connected to it. The composite moment was divided to two part, the first is the sum of the moment acting on each member (joist and Long. slab) separately and the second part, due to the axial force in each member was obtained by calculated as the difference of the joist thrust and the slab thrust multiplied by the lever arm between the point of application of the two forces (centroid of each element). For all figure a reference temperature was chosen to illustrate the level of heat reached by the structure at this stage of fire. The reference temperature is the temperature of the hottest steel region within the fire compartment, this was measured on the lower flange of the joist on grid line 2 (SB2_EF) at mid-span and thus this temperature is used in our text as the reference temperature.



Finite element model for fire test3

Figure 2

4. FIGURES DESCRIPTION

4.1. Heated joists

PBE__12

The primary Joist PBE__12 is 6m long, fixed between two columns. It has an I cross section type 356x171x51UB(50) with $\sigma_y=389\text{MPa}$, $\sigma_u=544$ and Elongation = 29(%). The column to beam connections is a standard connection using a flexible 8mm thick end plates of grade 43 steel and 8 grade 8.8 bolts with a 6mm fillet weld size. This connection is modelled as a pinned connection in the FE model.

Figure 3 shows the deflection at each section of the primary beam, two main pattern of behaviour can be noticed on the figure, a linear increase of deflection against temperature up to 690°C (first step1 in the model), followed by a non-linear increase of deflection till the end of the fire (step2). The good agreement with the test measurement on the deflection patterns was published elsewhere (Sanad 2000)¹³, here we can notice the homogeneous deflection over the whole length. Figure 4 to Figure 14 show the axial forces, shear forces, moment at each section of the individual elements of the beam (joist and composite slab). Also the total composite forces and moments at each section are presented to show the global behaviour of the composite beam.

SB12_EF

The edge secondary Joist SB12_EF is 9m long, fixed between two primary beams. It has an I cross section type 305x165x40UB(43) with $\sigma_y=389\text{MPa}$, $\sigma_u=544$ and Elongation = 29(%). The beam to beam connections is a standard connection using 10mm fin plate of grade 43 steel and 4 M20 grade 8.8 bolts with a 8mm fillet weld size. This connection is modelled as a pinned connection in the FE model.

Figure 15 shows the deflection at each section of this secondary beam, a linear increase of deflection against temperature up to the end of the fire is observed and we can notice the homogeneous deflection over the whole length. Figure 16 to Figure 26 show the axial forces, shear forces, moment at each section of the individual elements of the beam (joist and composite slab). Also the total composite forces and moments at each section are presented to show the global behaviour of the composite beam.

SB2__EF

The secondary Joist SB2__EF is 9m long, fixed between two columns. It has an I cross section type 305x165x40UB(43) with $\sigma_y=389\text{MPa}$, $\sigma_u=544$ and Elongation = 29(%). The column to beam connections is a standard connection using a flexible 8mm thick end plates of grade 43 steel and 8 grade 8.8 bolts with a 6mm fillet weld size. This connection is modelled as a pinned connection in the FE model. At 5m from the internal side the Joist is connected with another secondary Joist (254x146x31UB). The beam to beam connections is a standard connection using 10mm fin plate of grade 43 steel and 3 M20 grade 8.8 bolts with a 8mm fillet weld size. This connection is modelled as a pinned connection in the FE model.

Figure 27 shows the deflection at each section of this secondary beam, a linear increase of deflection against temperature up to the end of the fire and a homogeneous deflection over the whole length can be observed on the figure. Figure 28 to Figure 38 show the axial forces, shear forces, moment at each section of the individual elements of the beam (joist and composite slab). Also the total composite forces and moments at each section are presented to show the global behaviour of the composite beam. To be noticed that this beam has similar boundary condition to the heated secondary beam in Test1 (Sanad 1999)¹³.

4.2. Protected joists

PBF__12

The edge primary Joist PBF__12 is 6m long, fixed between two columns. It has an I cross section type 356x171x51UB(50) with $\sigma_y=389\text{MPa}$, $\sigma_u=544$ and Elongation = 29(%). The column to beam connections is a standard connection using a flexible 8mm thick end plates of grade 43 steel and 8 grade 8.8 bolts with a 6mm fillet weld size. This connection is modelled as a pinned connection in the FE model.

Figure 39 shows the deflection at each section of the protected edge primary beam, here we can notice the low value of deflections achieved at end of the fire. Figure 40 to Figure 50 show the axial forces, shear forces, moment at each section of the individual elements of the beam (joist and composite slab). Also the total composite forces and moments at each section are presented to show the global behaviour of the composite beam. To be noticed here that the axial forces developed in the protected joist are of relatively low magnitude compared to the yield capacity of the joist.

SB1__EF

The edge secondary Joist SB1__EF is 9m long, fixed between two columns. It has an I cross section type 356x171x51UB(50) with $\sigma_y=389\text{MPa}$, $\sigma_u=544$ and Elongation = 29(%). The column to beam connections is a standard connection using a flexible 8mm thick end plates of grade 43 steel and 8 grade 8.8 bolts with a 6mm fillet weld size. This connection is modelled as a pinned connection in the FE model.

Figure 51 shows the deflection at each section of the protected edge secondary beam, we can notice again the low value of deflections achieved at end of the fire. Figure 52 to Figure 62 show the axial forces, shear forces, moment at each section of the individual elements of the beam (joist and composite slab). Also the total composite forces and moments at each section are presented to show the global behaviour of the composite beam. Here the numerical model shows that the axial forces developed in the protected joist reaches the yield capacity of the joist near the connection with the column 1E.

4.3. Transverse slab

Rib at 0.9m from heated Primary beam

Figure 63 shows the deflection of the ribs situated at 0.9m from the heated primary beam at different instant during the fire. The curves show clearly a homogenous deflection over the whole width of the fire compartment, which increase also in a smooth manner with the temperature increase. Figure 64 show the moment developed in the ribs at different temperatures. Figure 65 show the shear forces over along the same rib, we can notice the increase of the shear forces imposed on the rib during the fire regime. Figure 66 show the membrane force developed along the rib during the fire. We can observe that the ribs is constantly in *compression* which increase with increasing temperature. In fact as the deflection at this zone (near the primary beam) is restricted, the temperature increase of the rib against the rest of the slab (cold and stiff part), and between the secondary beams (which can generate lateral restrain to the ribs expansion), produces alrge compressive forces in this rib as can be observed from the figure.

Rib at 4.5m from heated Primary beam

Figure 67 shows the deflection of the ribs situated at 4.5m from the heated primary beam at different instant during the fire. The curves show clearly a homogenous deflection over the whole width of the fire compartment, which increase also in a smooth manner with the temperature increase. Figure 68 show the moment developed in the ribs at different temperatures. Figure 69 show the shear forces over along the same rib, we can notice the increase of the shear forces imposed on the rib during the fire regime. Figure 70 show the membrane force developed along the rib during the fire. We can observe that the ribs is constantly in *tension* which increase with increasing temperature. In fact the deflection at this zone (mid-span of secondary beams) is large due to displacement compatibility within the slab plane. The temperature increase of the rib is not enough to supply the needed expansion to fit the deflected shape imposed by the longitudinal secondary beams, this produces large tension forces in this rib as can be observed from the figure.

Rib at 7.2m from heated Primary beam

Figure 71 shows the deflection of the ribs situated near the edge primary beam (7.2m from the heated primary beam) at different instant during the fire. The curves show clearly a homogenous deflection over the whole width of the fire compartment, which increase also in a smooth manner with the temperature increase. Figure 72 show the moment developed in the ribs at different temperatures. Figure 73 show the shear forces over along the same rib, we can notice the increase of the shear forces imposed on the rib during the fire regime. Figure 74 show the membrane force developed along the rib during the fire. We can observe that the ribs is constantly in *compression* which increase with increasing temperature. In fact as the deflection at this zone (near the primary beam) is restricted, the temperature increase of the rib against the rest of the slab (cold and stiff part), and between the secondary beams (which can generate lateral restrain to the ribs expansion), produces alrge compressive forces in this rib as can be observed from the figure.

5. CONCLUSION

Fire test3 was modelled using the grillage approach developed by Sanad⁹ et al. Different key features are observed from the analysis of the test results :

1. protected joists (secondary and primary) are subject to large plasticity during the fire.
2. The section nearer to the supports (connections) are the first one to reach yield, this happens for temperatures as low as 200°C.
3. Between 200°C and 500°C most joists are subject to yield axial forces along the whole lengths
4. Beyond 500°C the heated joist are subject to softening and the capacity of each joist reduces dramatically.
5. Although the above is the case for all heated joist, the structure doesn't suffer any serious instability or loss of integrity due to the large capacity of the slab which acts compositly with the joist to carry the imposed thermal loads during the fire.
6. The development of large compressive forces in the joist inside the heated compartment in test3 is in good agreement with the results obtained from other Cardington fire test (Sanad 1999)¹¹.
7. The membrane force are largely developed in the slab, specially in the short direction of the compartment (transverse direction here).
8. Two types of membrane forces are generated within the slab plan in the above direction tensile and compressive membrane forces.
9. Compressive membrane force are developed in the low deflection heated zones mainly near the primary beams (heated and edge one)
10. Tensile membrane forces are generated in the large deflection zone at mid-span of the secondary heated joists
11. The membrane actions in the slab's transverse direction are imposed by the displacement compatibility in the longitudinal and transverse directions.
12. The membrane action in the slab are largely produced between the secondary beams which give a support for this forces due to large in-plane stiffness of the composite slab on top of the joists.
13. The development of membrane action in the slab plan is in good agreement with the results obtained from other Cardington fire test (Sanad 1999)¹¹.

6. REFERENCES

1. Abaqus (1994): "Abaqus theory manual and users manual, version 5.4", Hibbit, Karlsson and Sorensen Inc., Pawtucket, Rhode Island, USA
2. P.N.R. Bravery (1993): "Cardington large building test facility, Construction details for the first building", internal report British Steel plc.
3. D.J. O'Connor and al. (1995): "Determination of the fire endurance of model concrete slabs using a plastic analysis methodology", The Structural Engineer, Volume 73, No 19/3.
4. Eurocode2 (1995): "Design of concrete structures Part1 2 : General rules Structural fire design", ENV 1992 1 2.
5. Eurocode3 (1995): "Design of steel structures Part1 2 : Fire resistance", ENV1993 1 2.
6. Eurocode4 (1994): "Design of composite steel and concrete structures Part1 1 : General rules and rules for buildings", ENV 1994 1 1.
7. B.R. Kirby (1995): "Behaviour of a multi storey steel framed building subject to natural fires: Test1 restrained beam, deflection measurements", Document ref; S423/1/Part D1, British Steel plc.
8. B.R. Kirby (1995): "Behaviour of a multi storey steel framed building subject to natural fires: Test1 restrained beam, against temperature measurements", Document ref; S423/1/Part T1, British Steel plc.
9. Sanad, A.M., Rotter, J.M., Usmani, A.S. and O'Connor, M.A. (1999) "Finite element modelling of fire tests on the Cardington composite building", Proc., Interflam '99, 8th International Fire Science and Engineering Conference, Edinburgh, 29 June - 1 July, Vol. 2, pp 1045 - 1056.
10. A.M. Sanad (1999): "British Steel Fire Test1: Reference ABAQUS model using grillage representation for slab", Research report R99 MD1, University of Edinburgh.
11. A.M. Sanad (1999): "British Steel Fire Test1: Analysis of results from BS/TEST1 model, Part A: Slab grillage model"
12. A.M. Sanad (2000): "British Steel Fire Test3: Reference ABAQUS model using grillage representation for slab", Research report R00 MD10, University of Edinburgh.

7. FIGURES